Proceedings of COBEM 2005
18th International Congress of Mechanical Engineering
November 6-11, 2005, Ouro Preto, MG

NUMERICAL SIMULATION OF THE FLOW AROUND A SPHERE USING THE IMMERSED BOUNDARY METHOD

Campregher, Rubens
Faculty of Mechanical Engineering, (FEMEC) - Federal University of Uberlândia (UFU)
38400-902 – Uberlândia - Brazil
campregher@mecanica.ufu.br

Silveira Neto, Aristeu
Faculty of Mechanical Engineering, (FEMEC) - Federal University of Uberlândia (UFU)
38400-902 – Uberlândia - Brazil
aristeus@mecanica.ufu.br

Mansur, Sérgio S.
Mechanical Engineering Department - UNESP Câmpus Ilha Solteira
15385-000 – Ilha Solteira - SP - Brazil
mansur@dem.feis.unesp.br

Abstract. *The numerical simulation of internal and external flows using the Immersed Boundary Methods allows the insertion of bodies by a force field added to the Navier-Stokes equations source term. The geometries are formed by a lagrangean mesh that overlaps, without interference, the eulerian mesh which the flow are been solved. This metodology permits, for instance, the complete independence of the lagrangean geometry, suitable for very complex flow simulation such as fluid-structure interaction. However, the evaluation of the lagrangean force field is not trivial, and several approaches are found in the literature. The Physical Virtual Model PVM, a methodology to obtain the lagrangean force field, has shown very competitive when compared against the traditional methods. In this work, an extension to the PVM to 3D domains is proposed and the classical flow around a sphere was chosen as a test case. The numerical code was written in Fortran 90 for an in-house Beowulf-class cluster with a MPI parallel library. The Navier-Stokes equations were implicit discretized by the Finite Volume Method in a spatial and temporal second order approximation. The results for flow field topologies and drag coefficients were compared against those in the literature, up to a Reynolds number of 1000.*

Keywords*: Immersed Boundary Method, Flow around a Sphere, Numerical Method, Low Reynolds Numbers*

1. Introduction

In the Immersed Boundary Methods, an interface inside a flow can be simulated by adding a force term inside the Navier-Stokes source term. Its initial development was due to Charles Peskin (1977) as an effort to simulate the blood flow through cardiac valves. In that work, the computational domain (having an Eulerian basis) was discretized by the Finite Differences method and the heart and the valves were modeled by a set of Lagrangian points. In order to promote resistance against the deformation imposed by the flow, those points were attached each other by strings. Thus, the tension expected when the strings are stretched was introduced on the flow momentum equation via source term, after it had been changed from a surface to a body force type.

It is very important to note that the Immersed Boundary Methods differentiates among them by the way the body force terms are obtained. In a later work of Lai (1998), higher order discretization techniques have been used, increasing the methodology numerical stability to the time step size. Later on, Roma *et al.* (1999) have reformulated the original model of Peskin introducing adaptive meshes and a new interpolation function.

An interesting application of the Immersed Boundary Method was its use in two-phase flows, as done by Unverdi & Tryggvason (1992). In that work, the authors simulated two and three-dimensional Finite Element represented bubbles inside a flow. The interfacial tension between the two-phase flows was, after applying a proper distribution function, inserted into the momentum equations as body force term. One of the authors' important contributions was to introduce an indicator function to locate the boundary inside the domain.

Goldstein et al. (1993) proposed a function that could bring the velocity of the flow particles adjacent to the geometry surface to the same velocity of the surface itself, creating a non-slip boundary condition, by using *ad-hoc* constants into the forcing terms. One of the constants produces a natural frequency oscillation, while the other one dumps the response oscillations. The authors have referred to their methodology as the *feedback forcing method* due to the fact that the constants are adjusted based on flow behavior as the force term is added into it.

The evaluation of the force field based on momentum balancing equation at the geometry surface was done by Mohd-Yusof (1997), which has avoided the use of *ad-hoc* constants. This methodology was named *direct forcing method* and despite diminished the problem dependence of the numerical formulation, has employed a quite expensive B – spline interpolation functions.

A comparison between Goldstein's and Mohd-Yusof's works can be found in Fadlun *et. al.* (2000). Their paper revealed that even with the more expensive procedure used in the *direct forcing method*, it has taken advantages over the *feedback forcing method*, especially in three-dimensional domains.

Kim *et. al.* (2001) have performed experiments employing the Mohd-Yusof's methodology on a Finite Volume discretized Eulerian domain, but using linear and bilinear interpolation techniques. Furthermore, the authors have changed the discretized mass conservation equation by inserting extra terms, based on volume fractions taken by the fluid, into its source term. That procedure has decreased the methodology dependence on grid point number inside the body and their relative distance from the volumes center.

Three-dimensional geometries generated by triangular Finite Element meshes inside flows discretized by cartesian grids were proposed by Gilmanov *et al*. (2003). However, the force terms are evaluated along to each mesh point normal line, requiring several decompositions and interpolations. In order to validate their methodology, the authors have performed simulations of the flow around a sphere at Reynolds number up to 300.

The methodology used in the present work was originally presented by Lima e Silva *et al.* (2003) and proposes to evaluate the forcing term by the momentum balance equation, as done by Mohd-Yusof. However, it employs a less expensive interpolation strategy. It is important to mention that the flow non-slip condition over the surface was not directly imposed, but is reached as the Lagrangian momentum balancing equations are being explicitly solved. Due to this quite different approach, the methodology was named *virtual physical method* (VPM).

This work proposal is to present a three-dimensional extension from the original two-dimensional VPM, having the Eulerian domain discretized by the Finite Volume Method and the geometry by a Finite Element mesh. Due to the fact that the Finite Element mesh allows construct very complex geometries, the capability of import and insert them into the domain, shows a very promising feature for the numerical code. The triangular elements that take part of the mesh act as basis to the Lagrangian set of points, as will be better seen further.

In order to validate the numerical code developed, the flow around a single sphere was chosen, based on numerical and experimental results drawn from Johnson & Patel (1999) and Ploumhans *et al.* (2002). The flow around spheres represents an interesting extension from the two-dimensional flow around circular cylinders. However, it promotes a much more complicated interaction among the three-dimensional flow structures and, despite its simple geometry, furnishes very rich information about the flow around bluff bodies.

2. Matematical Modeling

In order to better explain the methodology employed, the mathematical description of the procedure will be split in the Eurian domain and in the Lagrangian domain basis. Moreover, one of the most important characteristic presented by the method is that the flow in both domains has their properties evaluated separately. The linkage between them is done via interpolation functions. This feature enables the user to explore, for example, geometry movements inside the flow domain, once the two meshes are not connected. Thus, Fluid-Structure Interaction problems tend to become less expensive since the remeshing requirements, usually found in conventional methodologies, are no longer needed.

2.1. Eulerian domain

The Eulerian domain was discretized by a Cartesian non-uniform mesh since a body-fitted one isn't needed, as commented above. The Fig. 1 depicts the computational domain employed in the flow discretization. It is possible to see that grid was concentrated around the sphere region, that allows to improve the mesh resolution close to the geometry studied without excessively increase the computational resources needed. Even though, it is well-known that three-dimensional numerical simulation of flows tend to be computer memory glutton.

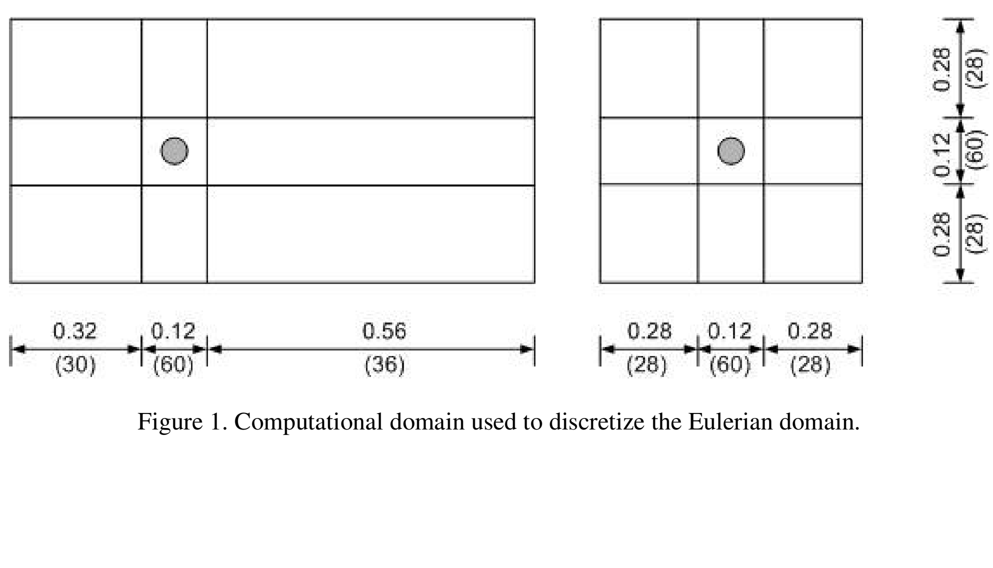

Figure 1. Computational domain used to discretize the Eulerian domain.

In order to remedy this, the Eulerian domain counterpart of the numerical code was written using parallel computing architecture. The strategy adopted was domain decomposition due to the hardware available in the laboratory: a Beowulf class cluster of PCs (Campregher *et al.*, 2004). Another possible way of doing that would be distributing the computational processes involved, as is usually done on vectorized machines (CRAY type, for instance). The partitioned domain and its respective meshes, cut halfway along the *y* axis, are depicted in Fig. 2. An important point to be stressed is that the Lagrangian domain and the Virtual Physical Model itself are not parallelized yet. Thus, the geometry studied must stay confined inside its specific subdomain. It is known by the authors that this could sound a little restrictive, and a lot of effort has been put to cope with this.

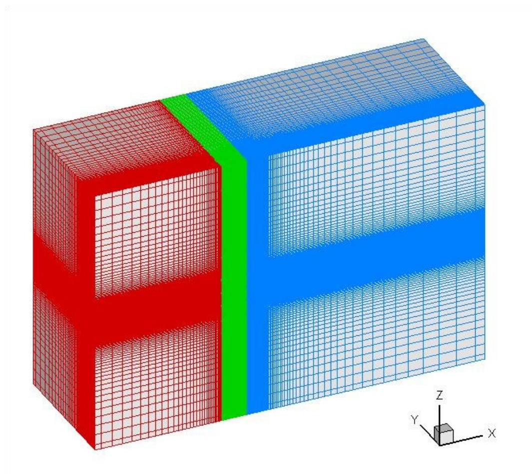

Figure 2. Computational subdomains due to the parallel computing strategy.

The computational domain was discretized by Finite Volume method and the flow was considered incompressible and isothermal. Thus, the Navier-Stokes equation in its integral form can be written as:

$$\frac{\partial}{\partial t}\int_{\Omega}\rho u_i d\Omega+\int_{S}\rho u_i v\cdot ndS=\int_{S}\tau_{ij}i_j\cdot ndS-\int_{S}pi_j\cdot ndS+\int_{\Omega}f_i d\Omega, \tag{1}$$

where ρ is the constant density, fi is the force field term associated with the Volume Element i, τ_{ij} *ij* is the viscous term, and the p_i *i* is the pressure. The time derivative was discretized by the three-time level approximation, having second-order accuracy (Ferzinger and Perić, 2002) and the advective terms was discretized by the Central Difference Scheme (CDS).

The pressure-velocity coupling was done by the SIMPLEC method with no relaxation in the velocity components equation. A co-located arrangement of the variables was employed and the Rhie-Chow (Rhie and Chow, 1983) interpolation method was used to avoid numerical oscillation due to pressure checkerboard fields. As the Cartesian mesh was not fine enough to keep the solution stable when using CDS interpolation in the advective terms, a deferred-correction algorithm was implemented. Thus, an upwind interpolation was blended with a CDS one by:

$$\left(F\right)^n=\left(F_L\right)^n+\gamma\left(F_H-F_L\right)^{n-1}, \tag{2}$$

where *L* and *H* means, respectively, low and high order flux term and *n* is the current iteration. A value of $\gamma = 1.0$ was used in all tests.

The linear system generated by the velocity components discretization was solved by the SOR (Successive Over-Relaxation) algorithm whereas the SIP (Strongly Implicit Procedure) algorithm was employed to solve the pressure correction system of equations.

2.2. Lagrangian domain

In the Immersed Boundary Method, only the geometry surface is of interest. Thus, the Finite Element mesh represented only the sphere border as can be seen in Fig. (3a). The centroid of the triangular elements is the locus of the Lagrangian point *k* associated with this element of surface area ΔA_k and average perimeter ΔS_k. Moreover, each of the points has a normal vector $\mathbf{n}_k$ associated that points outwards, as depicted in Fig. (3b). The coordinates of the P_1,P_2, and P_3 points that form the triangular element in Fig. (3b) allows one to evaluate the element area by using the following relation:

$$\Delta A_k = \sqrt{S(S-S_1)(S-S_2)(S-S_3)}, \tag{3}$$

where $S_1 = \overline{P_2P_1}$, $S_2 = \overline{P_3P_2}$, $S_3 = \overline{P_3P_1}$, and $S = (1/2)(S_1 + S_2 + S_3)$.

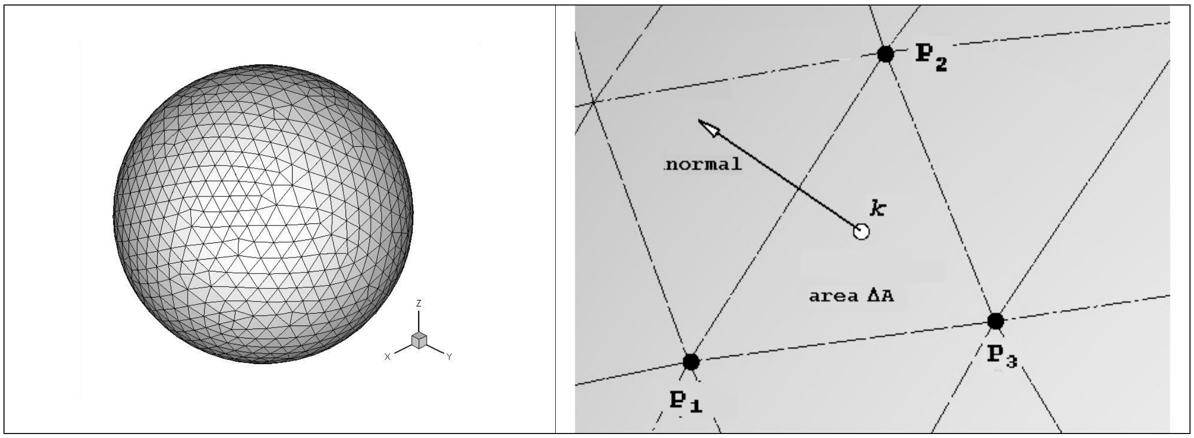

Figure 3. Finite Element mesh for the sphere discretization (left) and the detailed view of the Lagrangian point k inside the triangular element.

Applying the momentum equation to each k Lagrangian particle of fluid one has:

$$F_{i,k} = \frac{u_{i,k} - u_{i,fk}}{\Delta t} + \frac{\partial\left(\rho u_{j,k} u_{i,k}\right)}{\partial x_{i,k}} - \mu\left[\frac{\partial}{\partial x_{i,k}}\left(\frac{\partial u_{i,k}}{\partial x_{i,k}}\right)\right] + \frac{\partial p_{i,k}}{\partial x_{i,k}}, \tag{4}$$

where $F_{i,k}$ is the force, along the direction i, needed to change the velocity of the fluid particles adjacent to the Lagrangian point k, to attain the wall velocity $u_{i,k}$, i.e., performing the non-slip condition at the geometry wall.

2.3. The Physical Virtual Model

Since the way of each Immersed Boundary Methodology evaluates the f_i term in Eq. (1) differentiates it each other, the Physical Virtual Method characterizes by isolating the Lagrangian force F_k from the momentum equation in a point k of the Eq. (4). In sequence, the model promotes the interpolation of each force to its surrounding volume Ω_i in the Eulerian domain, weighted by their relative distances by a distribution function D_i. In a mathematical formulation, one can represent this operation by:

$$f_i = \sum_k F_{i,k} D_i \Delta A_k \Delta S_k \tag{5}$$

The distribution function is evaluated as:

$$D_i\left(x_k\right) = \prod\left\{\frac{\varphi\left[\left(x_k - x_i\right)/\Delta x_i\right]}{\Delta x_i}\right\}, \tag{6}$$

where the φ function is defined as:

$$\varphi(r) = \begin{cases} \tilde{\varphi}(r) & se\ \|r\| < 2 \\ \frac{1}{2} - \tilde{\varphi}(2-r) & se\ 1 < \|r\| < 2, \\ 0 & se\ \|r\| > 2 \end{cases} \tag{7}$$

and:

$$\tilde{\varphi}(r) = \frac{3 - 2\|r\| + \sqrt{1 - 4\|r\| - 4\|r\|^2}}{8} \tag{8}$$

One can see that the Distribution function cancels out the influence of Lagrangian points placed at distances greater than 2 cells. This value was previously studied and proved to be sufficient to maintain the methodology accuracy. Thus, once the F_k force is calculated from Eq. (4), it is interpolated to the related elementary volume by the Eq. (5) forming the Eulerian forcing term f_i, which is added to the Navier-Stokes equations as represented in Eq. (1). After the flow equations has been solved, the outer iteration is completed and the solution advances in time.

3. Results and Discussion

The simulations were performed for several Reynolds numbers, defined in function of the free stream velocity U_∞ and sphere diameter D, ranging from 100 to 1000 in steps of 100. The domain dimensions are as shown in Fig. 1, i.e., X_{max} = 1.00m, $Y_{max} = Z_{max}$ = 0.68m. It was employed in the x, y, and z directions, respectively, 126x118x118 grids that results in about 1.75 million of volumes. The domain boundary conditions were set as follows: free-slip in the side walls, constant velocities of $U = U_\infty$ and V = W = 0.0m/s in the input, and zero derivatives for all variables in the output.

For the surface discretization was employed 1892 triangular elements, forming a sphere of diameter D = 0.04m and center placed at (x_c,y_c,z_c) = (0.38, 0.34, 0.34)m. The dimension of the sphere and the Eulerian domain gives a blockage ratio of 0.27%, which is enough to avoid any interference on the results.

The Figure 4 shows the streamlines pattern at Reynolds numbers of 100 (Fig. 4a), 200 (Fig. 4b), 300 (Fig. 4c), 500 (Fig. 4d), and 1000 (Fig. 4e). Observing the difference between the patterns in the Fig. 4b and 4c, is possible to recognize the transition onset that starts within 275 < Re < 295 accordingly to the literature (Gushchin *et al.*, 2002). In the Figs. 4d and 4e is possible to see the streamline patterns at higher Reynolds showing a quite more chaotic behavior, which is reported to be Re > 420 (Tomboulides and Orszag, 2000). At these high regimes, the symmetry observed in the Figs. 4a,b or even the permanence of the streamlines along the sphere equator plane are no longer possible.

In order to better study the vortex shedding phenomena, it was employed the Q criteria (Jeong and Hussain, 1995), defined as:

$$Q = \frac{1}{2}\left(\|\Omega\|^2 - \|S\|^2\right) \tag{9}$$

where $\|S\| = [tr(SS^T)]^{1/2}$ and $\|\Omega\| = [tr(\Omega\Omega^T)]^{1/2}$. The **S** and **Ω** are the symmetric and antisymmetric parts of ∇u.

The Fig. 5 represents the Q = 0.8 isovalues for flow at Re = 400 in four different times in sequence (from Fig. 5a to Fig. 5d). Thus, is possible to see the hairpin vortex formation and the shedding behind the sphere. It worth noting the alternating shed feature, characteristic of this class of flows.

The drag coefficient was also evaluated based on the x component of the Lagrangian force (F_x), and compared against the data from literature (Fornberg, 1988) and from correlations, as depicted in Fig. 6. It was calculated as:

$$C_D = \frac{Fx}{\left(\frac{1}{2}\right)\rho U_\infty^2 \left(\frac{\pi D^2}{4}\right)} \tag{10}$$

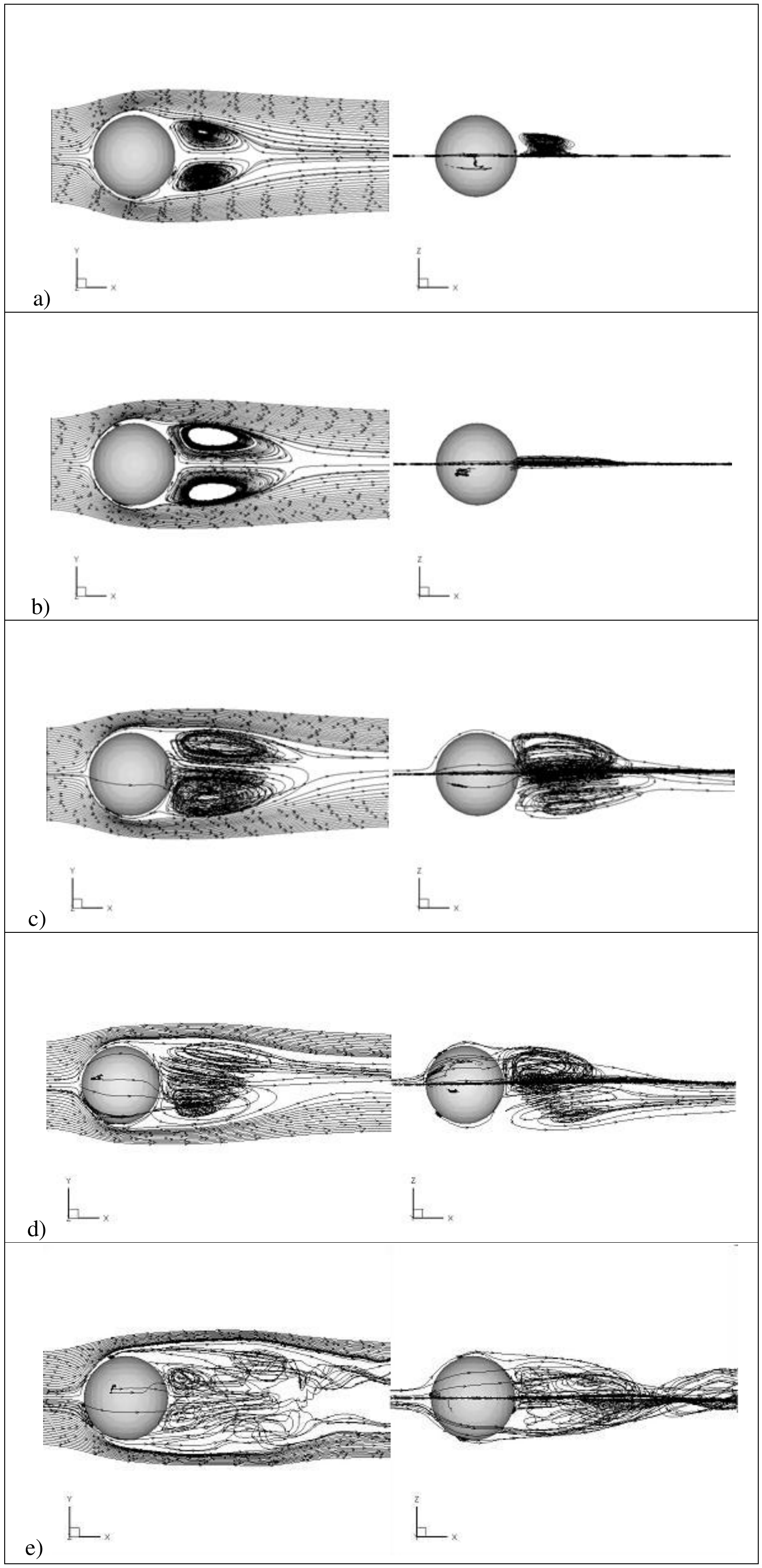

Figure 4. Streamline patterns at Re = 100 (a), 200 (b), 300 (c), 500 (d), and 1000 (e).

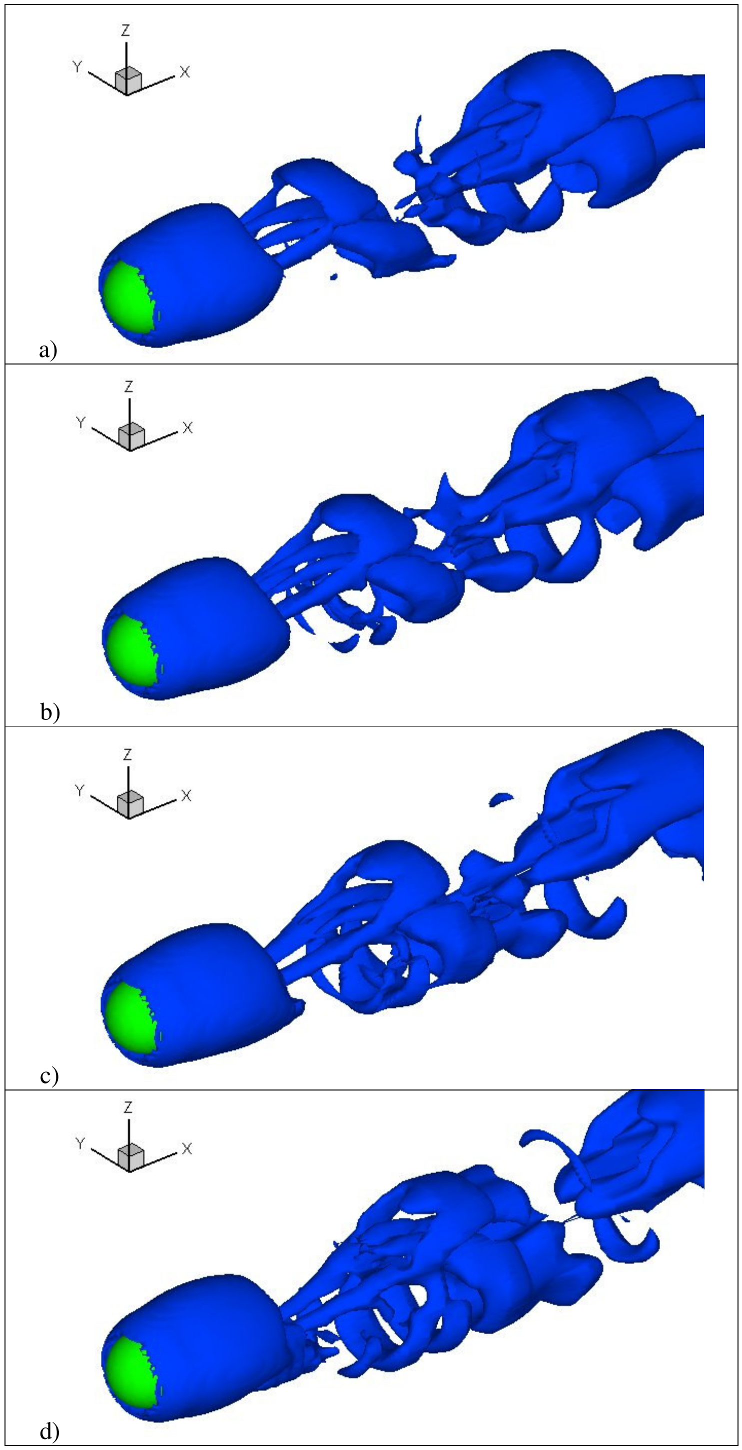

Figure 5. Isovalues of Q = 0.8 at Re = 400 for four different time shots.

4. Acknowledgements

The authors would like to thank the CAPES and CNPq Agencies for the financial support.

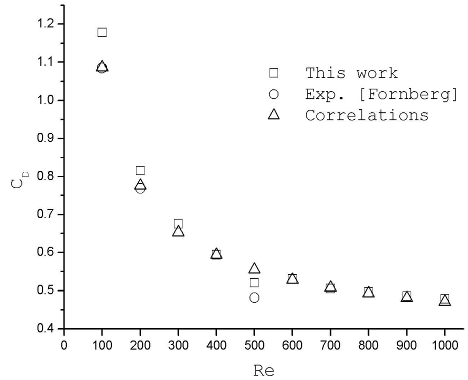

Figure 6. Drag coefficients compared against the data from literature and correlations.

5. References

Campregher, R., Silveira Neto, A., Marinho, W.P., and Mansur, S.S., 2004, “Numerical Simulation of the backward-facing step in a Beowulf-class cluster”, In proceedings of the XXI ICTAM – International Congress of Theoretical and Applied Mechanics, Warsaw, Poland.

Fadlun, E., Verzicco, R., Orlandi, P., and Mohd-Yusof, J., 2000, “Combined immersed-boundary finite-difference methods for three-dimensional complex flow simulations”, J. Comp. Phys. vol. 161, p.35.

Ferziger, J. and Peric, M., 2002, “Computational methods for fluid dynamics”, 3rd ed., Springer-Verlag, New-York, USA.

Fornberg, B., 1988, “Steady viscous flow past a sphere at high Reynolds number”, J. Fluid Mech. vol. 190, p. 471.

Gilmanov, A., Sotiropoulos, F., and Balaras, E., 2003, “A general reconstruction algorithm for simulating flows with complex 3D immersed boundaries on cartesian grids”, J. Comp. Phys. vol. 191, pp. 660.

Goldstein, D., Handler, R., and Sirovich, L., 1993, “Modeling a no-slip flow boundary with an external force field”, J. Comp. Phys. vol. 150, p. 354.

Gushchin, V., Kostomarov, A., Matyushin, P., and Pavlyukova, E., 2002, “Direct numerical simulation of the transitional separated fluid flows around a sphere and a circular cylinder”, J. Wind Eng. and Ind. Aerodynamics vol. 90, p. 341.

Jeong, J. and Hussain, F., 1995, “On the identification of the vortex”, J. Fluid Mech. vol. 285, pp.69-94.

Johnson, T.A. and Patel, V.C., 1999, “Flow past a sphere up to a Reynolds number of 300”, J. Fluid. Mech. vol. 378, pp. 19-70.

Kim, J., Kim, D., and Choi, H., 2001, “An immersed-boundary finite-volume method for simulations of flow in complex geometries”, J. Comp. Phys. vol. 173, p. 636.

Lai, M.C., 1998, “Simulations of the flow past an array of circular cylinders as a test of the Immersed Boundary Method”, Ph.D. Dissertation, New York University, NY

Lima e Silva, A.L.F., Silveira-Neto, A., and Damasceno, J.J.R., 2003, “Numerical simulation of two dimensional flows over a circular cylinder using the immersed boundary method”, J. Comp. Phys. vol. 189, p. 351.

Mohd-Yusof, J., 1997, “Combined immersed boudaries/B-splines methods for simulations in complex geometries”, CTR Annual Research Briefs, NASA Ames/Stanford University.

Peskin, C.S., 1977, “Numerical analysis of the blood flow in the heart”, J. Comp. Phys. vol. 25, p. 220.

Ploumhans, P., Winckelmans, G.S., Salmon, J.K., Leonard, A., and Warren, M.S., 2002, “Vortex methods for direct numerical simulation of three-dimensional bluff body flows: application to the sphere at Re = 300, 500 and 1000”, J. Comp. Phys. vol. 178, pp. 427-463.

Rhie, C. and Chow, W., 1983, “Numerical study of turbulent flow past an airfoil with trailing edge separation”, AIAA Journal 21, 1525.

Roma, A., Peskin, C.S., and Berger, M., 1999, “An adaptive version of the immersed boundary method”, J. Comp. Phys. vol. 153, p. 509.

Tomboulides, A.G. and Orszag, S.A., 2000, “Numerical investigation of transitional and weak turbulent flow past a sphere”, J. Fluid Mech. vol. 416, p.45.

Unverdi, S., Tryggvason, G., 1992, “A front-tracking method for viscous, incompressible multi-fluid flows”, J. Comp. Phys. vol. 100, p. 25.

6. Responsibility notice

The authors are the only responsible for the printed material included in this paper.